SEGMENTING DERMOSCOPY IMAGE WITH DIFFERENT IMAGE PROCESSING ALGORITHMS

by

Shakar Hussein SALIH

A thesis submitted to

The Graduate School of Sciences and Engineering

of

Fatih University

In partial fulfillment of the requirements for the degree of

Master of Science

in

Computer Engineering

Feb 2016
Istanbul, Turkey

APPROVAL PAGE

This is to certify that I have read this thesis written by Shakar Hussein SALIH and that in my opinion it is fully adequate, in scope and quality, as a thesis for the degree of Master of Science in Computer Engineering.

_____
Assist. Prof. İhsan H. AKIN
Thesis Supervisor

_____
Assist. Prof. Saime A. AKAR
Thesis Co-Supervisor

I certify that this thesis satisfies all the requirements as a thesis for the degree of Master of Science in Computer Engineering.

_____
Assist. Prof. Kadir TUFAN
Head of Department

Examining Committee Members

Assist. Prof. İhsan H. AKIN _____

Assist. Prof. Saime A. AKAR _____

Assist. Prof. Kadir TUFAN _____

Assist. Prof. Birol TİLKİ _____

Assist. Prof. Mustafa ŞANVER _____

It is approved that this thesis has been written in compliance with the formatting rules laid down by the Graduate School of Sciences and Engineering.

_____
Prof. Nurullah ARSLAN
Director

February 2016

SEGMENTING DERMOSCOPY IMAGE WITH DIFFERENT IMAGE PROCESSING ALGORITHMS

Shakar Hussein SALIH

M. S. Thesis - Computer Engineering
Jan 2016

Thesis Supervisor: Assist. Prof. Dr. Ihsan AKIN

Co-Supervisor: Assist. Prof. Dr. Saime AKAR

ABSTRACT

Melanoma is the most common dangerous type of skin cancer. On the other hand, if found in an early stage, there is a high likelihood of cure. For that reason, various types of imaging techniques have been investigated. Dermoscopy is one non-invasive imaging technique for diagnosis. The accuracy of diagnosis using dermoscopy is very important and depends on the experience of dermatologists. Visual examination is a waste of time, so there is currently wide attention paid to the development of computer-aided diagnostic systems to aid the clinical evaluation of dermatologists. Image Segmentation is very important in digital-image processing and self-discovery, with an important role to play in solving many difficult problems, particularly those related to chronic diseases, such as skin cancer. Analysis of automatic dermoscopy images usually has three stages: a) feature selection and extraction, b) image segmentation, and c) feature classification. Here, we suggest and test three methods that are applied to 22 dermoscopy images: a) active contour modeling, b) the level set method, and c) a proposed method of fuzzy clustering based on region growing. We evaluated our methods using three metrics; our proposed method of fuzzy clustering based on region growing achieved the best ratio.

Key words: Image Segmentation, Dermoscopy, Skin Lesion.

DERMOSKOPİ GÖRÜNTÜLERİNİN FARKLI GÖRÜNTU İŞLEME YÖNTEMLERİ İLE BÖLÜTLENMESİ

Shakar hussein SALIH

Yüksek Lisans Tezi- Bilgisayar Mühendisliği
Jan 2016

Tez Danışmanı: Yrd. Doç. Ihsan AKIN

Eş Danışman: Yrd. Doç. Saime AKAR

ÖZ

Melanom cilt kanserleri arasında en tehlikelisi olmakla birlikte erken tanısı sonucunda yüksek tedavi olasılığına sahiptir. Bu nedenle farklı görüntüleme teknikleri kullanılarak incelenmektedir. Bunlar arasında girişimsel olmayan dermoskopik görüntüler tanı için kullanılanlardan biridir. Ancak, dermoskopik görüntülerdeki tanı başarısı dermatoloğun tecrübesine bağlı kalmakta ve çoğu zaman uzun sürmektedir. Bu nedenle, bilgisayar destekli tanı sistemleri kullanılarak klinik değerlendirmeye yardımcı araştırmalar son yıllarda artış göstererek dikkat çekmektedir. Önemli bir görüntü işleme adımı olan görüntü bölütleme cilt kanseri gibi çoğu hastalıkta oldukça zor problemleri çözmede önemli bir rol oynamaktadır. Otomatik olarak dermoskopik görüntülerini incelemek 3 aşamadan oluşmaktadır: a) öznitelik bulma, b) görüntü bölütleme, ve c) öznitelik sınıflandırma. Bu tez kapsamında, 22 dermoskopik görüntü 3 yöntem kullanılarak bölütleme başarısı açısından incelenmiştir. Bunlar, aktif kontor, level set ve bölge genişlemeli fuzzy yöntemleridir. Sonuçlar 3 objektif metrik kullanılarak değerlendirilmiş ve en başarılısının önerdiğimiz bölge genişlemeli fuzzy yöntemi olduğu belirlenmiştir.

Anahtar Kelimeler: Görüntü bölütleme, dermoskopi, cilt kanseri.

To my parents

ACKNOWLEDGEMENT

I want to thank to Assist. Prof. Dr. İhsan AKIN for his lead and insight throughout the thesis.

I express sincere thanks to my advisor Assist. Prof. Dr. Saime AKAR. I am honored to have had the chance of having her as my advisor. Without her this research would not have been possible.

My deepest gratitude goes to my parents and siblings for their love and unconditional support throughout my life and my studies. Made me live with a dream that has made me who I am now!

Finally, I would like to thank to all of my friends who helped me during this journey and made a memorable event.

TABLE OF CONTENTS

LIST OF TABLE

TABLE

LIST OF FIGURES

FIGURE

LIST OF SYMBOLS AND ABBREVIATIONS

SYMBOL/ABBREVIATION	
BCC	Basal Cell Carcinoma
DIP	Digital Image Processing
FCR	Fuzzy Clustering based on Region Growing
FN	False Negative
FP	False Positive
GVF	Gradient Vector Flow
MRI	Magnetic Resonance Imaging
MT	Multilevel Thresholding algorithm
SCC	Squamose Cell Carsinoma
SRM	Statistical Region Merging
TN	True Negative
TP	True Positive
UV	Ultraviolet

CHAPTER 1

INTRODUCTION

1.1 BACKGROUND

Skin cancer is among the most common types of human cancers [1]. There are two types of skin cancer; Melanoma and non-Melanoma. Because of the increasing rate of skin cancer, this problem is recognized at national and international levels. The government of UK aims to stop the rise of cancer [2].

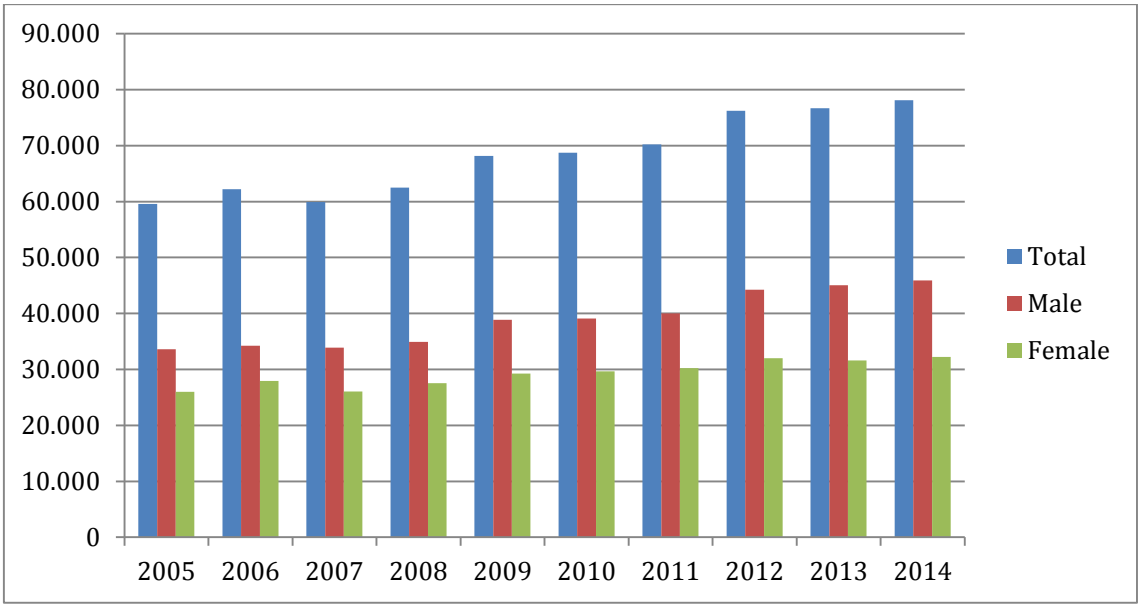

Figure 1.1 The rate of new melanoma cases every year in the United States from 2005 to 2014 [3].

In the United States, the appropriate terms for non-melanoma are basal-cell carcinoma (BCC) and squamous-cell carcinoma (SCC). According to the National Cancer Institute, in 2012, more than 2,000,000 new cases of squamous- and basal-cell carcinoma were diagnosed in the United State. The reason for such a wide range of estimates is that many early skin-cancer lesions are easily treated. Malignant Melanomas may be removed easily with an excellent prognosis [3].

To effectively detect skin cancers at an early stage without taking any skin biopsies, which was necessary, today digital image segmentation has been suggested using dermoscopy, photography, infrared thermal imaging, spectral imaging, and magnetic resonance imaging (MRI) [4]. Among these current imaging techniques, dermoscopy is the most suitable for diagnosing melanoma.

Dermoscopy is an imaging technique for diagnosis that is not invasive, used for bodily examination of pigmented skin lesions in dermatology. According to dermatologists in National Institute of Health, dermoscopy imaging has awesome potential to detect malignant melanoma at an early stage but it is time-wasting and subjective to Dermatologist. So, there is now wide attention to the development of diagnostic systems that are computer-aided in order to help analyze skin lesions [5]. Automatic analysis of dermoscopy images includes three main steps;

a) Feature selection and extraction

b) Image segmentation, and

c) Feature classification.

Among these three main steps, image segmentation plays a major role in digital-image processing, self-discovering the details of objects in important areas. This technique also has an important role to play in solving many difficult problems; such as object detection**,** recognition tasks, particularly those related to many chronic diseases, and skin cancer [6].

1.2 STATEMENT OF THE PROBLEM

Image segmentation is a major part of image processing, used in many important applications. Skin cancer is the most common of all cancers detected every year [22] According to results from Washington and Leaver, the rate of cancer is increasing [3]. Identifying skin cancer at an early stage is very important issue. Skin cancer can be detected by skin biopsies. The cost and time of this procedure is a problem. In order to reduce the cost and time required for detecting skin cancer, digital image segmentation is investigated as a means of diagnosis. If skin images can be segmented accurately by diagnosis, it will be good [7]. Lesions have a different form in terms of color, size, and irregular boundaries. It sometimes is smooth between the lesion and the skin, as a result the segmentation will be very hard [5]. Therefore, in our research, concentrated this problem. We suggested a new method and tested with two other methods for the segmentation of dermoscopy images of skin lesions, trying to find the best result for early detection.

1.3 PURPOSE OF THE STUDY

Many researchers have used segmentation methods to detect and analyze images [5, 6, 7]. Selveria, et al. [5], have also compared these methods to show which are better and faster at detecting cancer. They have used preprocessing, segmentation, feature extraction, and post-processing techniques to obtain accurate results.

The goal of this study is to compare three methods of segmentation for the early detection of skin cancer. We evaluated an active contour model, the level set method, and a new, proposed algorithm which combines fuzzy (C-mean) clustering and image region growing. This latter method was applied before to MR brain images [43]. We applied our methods to 22 dermoscopy images of melanoma-type lesions. These methods have not been compared together in any previous study. Three different metrics were applied to evaluate the methods of segmentation;

a) Specificity: true positive

b) Sensitivity: true negative

c) Accuracy: proportion of correctly identified over total samples.

1.4 THESIS OVERVIEW

The thesis overview is given in Figure 1.2. My study consists of three main stages.

The first stage is the preprocessing stage. In this step, the methods of segmentation have been applied to images of skin lesions after converting all images to grayscale.

The second step is the segmentation and extracting their success ratios under a framework. In this step, we propose a new method (fuzzy clustering based on region growing) and will compare with other two methods of segmentation (active contour modeling, and the level set method). These methods are detailed in Chapter 3.

In the last step, we examine the comparative results of the previous steps.

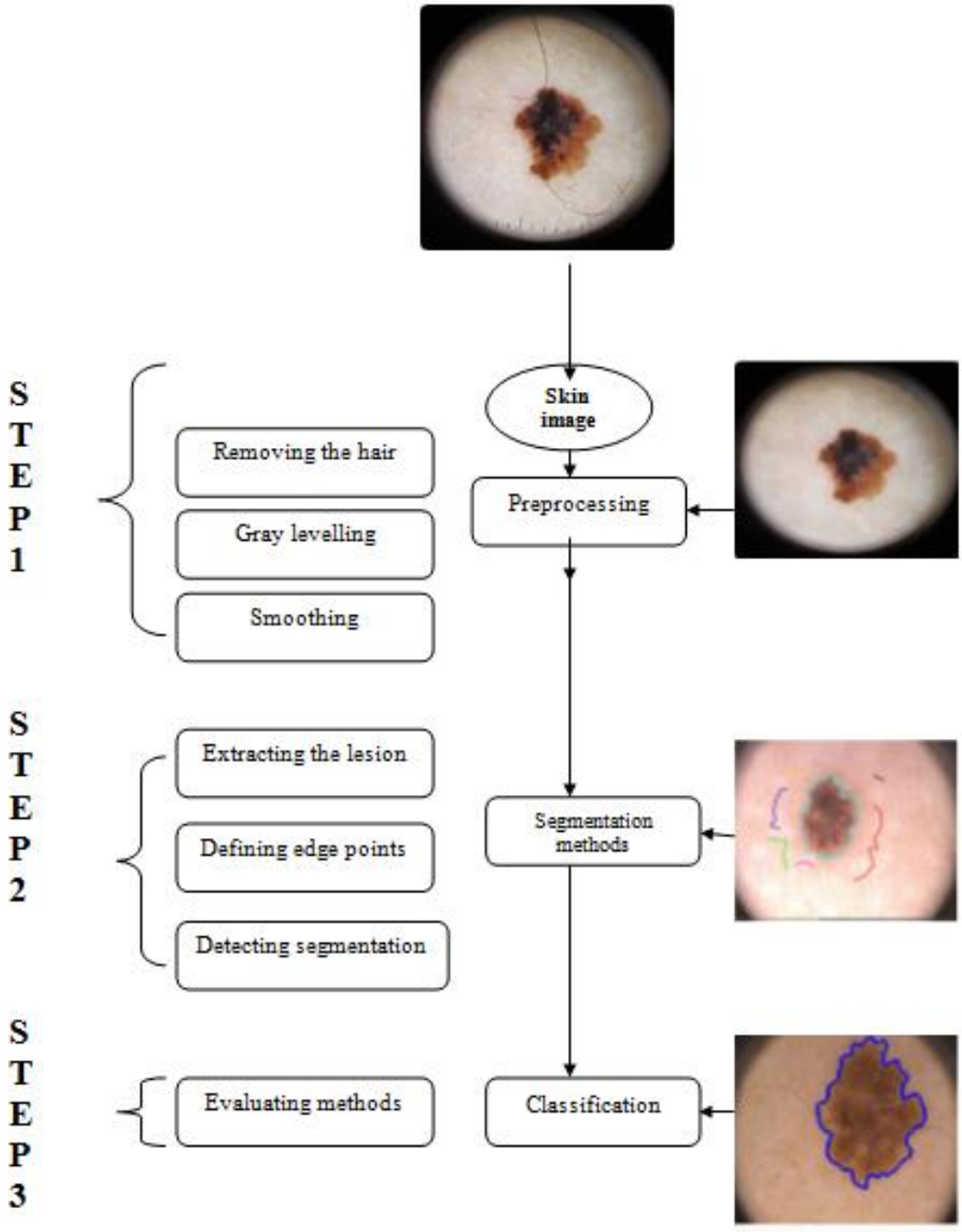

Figure 1.2 General Block Diagram of Segmentation in this Study

CHAPTER 2

LITERATURE REVIEW

2.1 SKIN

The largest organ in the human body is the skin, comprising 15% of total body weight in humans. Skin has several fundamental functions. It protects against external physical, chemical, and biological attackers, avoids additional water loss from the body, and has the responsibility of thermoregulation [8].

2.1.1 Skin Tissue Types

Skin is composed of three layers as follow:

1. **Epidermis:** The epidermis is the outermost layer of skin. It is made of flat cells named squamous cells. Under the squamous cells in the inner part of the epidermis are the basal cells. Melanocytes cells are distributed amongst the basal cells. They are located in the most inner part of the epidermis. Melanocytes create the skin color. In case of ultraviolet radiation explosion melanocytes generate more pigment and cause darkness of the skin.
2. **Dermis:** This is the middle layer that located between the epidermis and subcutaneous layer. It contains connective tissue in the form of collagen in bulk and elastin in minimal quantities, with a rich intertwining blood supply. The cells that are found in the dermis are fibroblasts, mast cells and histocytes. Dermis also contains hair follicles, nerves, lymphatic vessels and sweat glands.
3. **Hypodermis:** They are also called as subcutaneous tissue is the deepest layer mostly composed of fat which protects the skin from injury, produces heat. It is like a cushion for the body [9].

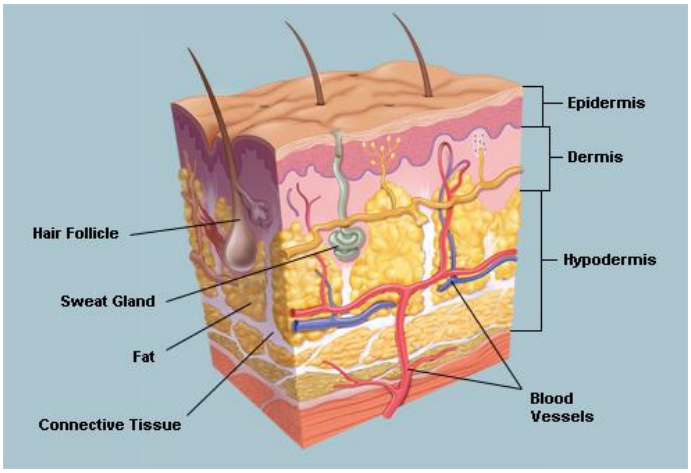

Figure 2.1 The types of skin tissue in three layers: the Epidermis, Dermis, and Hypodermis [10].

2.1.2 Types of Skin Cancer

We can classify the skin cancer into three groups in which only Melanoma is dangerous:

- **Basal-cell skin cancers (basal-cell carcinomas):** This type of skin cancer is very common cancer and therefore it considered very important. Eight of 10 skin cancers are basal-cell carcinomas (known as basal-cell skin cancers).
- **Squamous-cell skin cancers (squamous-cell carcinomas):** Two of 10 skin cancers are squamous-cell carcinomas.
- **Melanoma begins in melanocytes (pigment cells):** Melanoma starts in melanocytes; since most of these are in the skin, melanoma can be on any skin surface. In affected men, it is often seen in the head, neck, between the shoulders, and hips. However, in affected women, it is often seen in the lower area of the leg, between the shoulders, or the hips. People with darker skin colors rarely face melanoma, but if the disease develops in them, it mostly starts under the fingernails, toenails, and palms of the hand or feet [10].

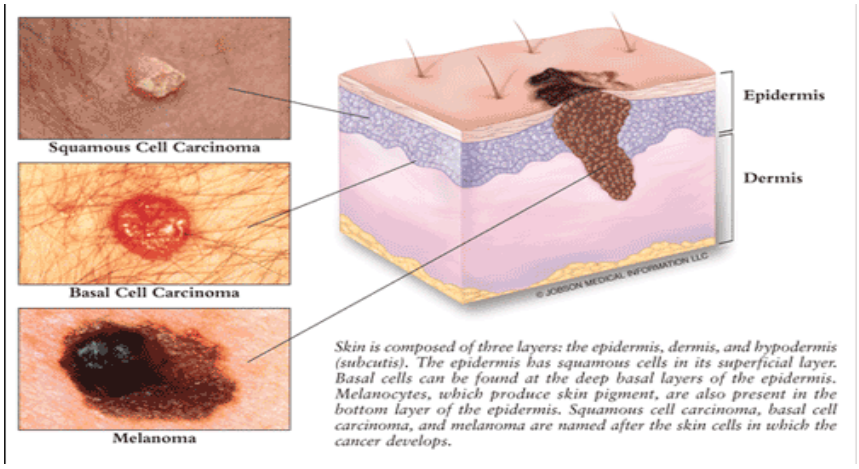

Figure 2.2 Types of skin cancer [10].

2.1.3 Causes of Skin Cancer

There are various factors of skin cancer such as age, genetics and facing some risk factors and life style factors as listed in [10].

- In the United Kingdom, 86% predictable malignant melanoma, the core factor of skin cancer, is caused by ultraviolet radiation of the sun.
- Added to that cause also the UV radiation of sunbeds, ionizing radiation, specific occupational contacts and certain health conditions and treatments.
- More than 8 in 10 males and nearly 9 in 10 females continue to have a malignant melanoma minimum of 10 years.
- If melanoma is diagnosed early 25% of females and 8% of males has five year survival duration.
- Non- melanoma skin cancer is the most common type; since it is diagnosed with early stage they do not cause life risk.
- The risk for skin cancer varies with skin type, hair and eye color, and number of moles.

.

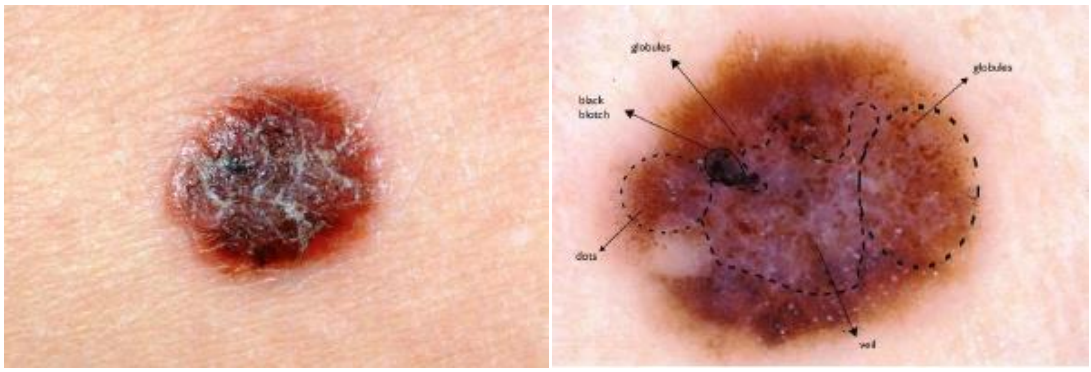

(a) (b)

Figure 2.3 a) An image of a lesion under clinical view (naked eye). b) The same lesion under dermoscopy with oil immersion. Images taken from [12].

Figure 2.3a shows a skin lesion under clinical view (the naked eye), while 2.3b shows the same skin lesion under dermoscopy covered by oil. Important features are marked, so malignant or benign lesions can be better diagnosed under dermoscopy.

2.2 DERMOSCOPY AND HISTORICAL BACKGROUND

In order to improve the medical diagnosis of melanoma light based visual technologies were used for the first time in 1990s [12]. Dermoscopy is a technique which lets in analyzing the colors and microstructures of epidermis, papillary dermis and dermal epidermal junction that can't be seen by the naked eye. When skin is evaluated by dermoscopy and analyzed using a particular optical system, the colored skin lesion is immersed with a liquid. Covering the skin with liquid helps in minimizing the reflection of the skin and improves of clearness of the stratum corneum. As a result, explicit structures that belong to the epidermis, papillary dermis and dermal epidermal junction is seen. Also, it indicates the area of melanin spreading.

Lately dermoscopy with Led Light with polarization is invented and by using polarized light it is not needed to cover the skin with a liquid, also some of the tools do not supposed to contact the skin directly. Non polarized light with polarized light and contact with non-contact dermoscopy differ in showing the tested lesions according to color and picturing the vessels. Benvenuto-Andrade et al. state that there is an agreement on most dermoscopic colors except blue-white shading and pink color when

polarized and non-polarized light is compared [11]. At the end of their report they also concluded that there is a reasonable agreement on the structure of dermoscopic image except the of milia-like cysts and comedo-like openings, these two are better imaged using non polarized light and polarized light, particularly when used with non-contact dermoscopy increases the visualization of vessels and red regions [12].

2.2.1 Types of Dermoscopy

There are two types of dermoscopy, analogue dermoscopy and digital dermoscopy.

(a) **(b)**

(C) **(d)**

(e)

(f)

(g)

Figures 2.4 a, b, e, and f show analogue dermoscopy. All of them, except the one shown in f, are attachable to digital cameras to function as digital dermoscopy. Figures 2.4 g, d, and c shown modern digital dermoscopy [12].

2.3 DIGITAL IMAGE PROCESSING (DIP) OF SKIN-LESION IMAGES

The main steps in the diagnosis of melanoma using computer-vision are;

a) acquisition image of skin,
b) segmentation,
c) location the region of the skin lesion,
d) extraction of features, and
e) Feature classification.

Segmentation detects the border of the lesion, separating it out in order to simplify diagnosis. Feature extraction automatically extracts the lesion from the skin, like a

manual extraction done by a dermatologist. This accurately distinguishes a melanoma lesion.

2.4 LITERATURE REVIEW

For medical diagnoses and analysis, extraction of melanoma from an image of a skin lesion plays an important role. Early detection will save many people's lives. Classical medical techniques are not enough to detect this dangerous disease. Current advancement in technology can play a role in detection. One way to clearly detect or show the image of cancer is segmentation. Many methods of segmentation have been investigated for these purposes, comprising four main types: thresholding, edge-based, region-based, and clustering-based. Many researchers have been working on computer-vision approaches to skin-cancer detection. In order to segment skin lesions in the input image, existing systems use manual, semi-automatic, or fully automatic modes.

A wide ranging study of different methods has been applied to segmentation of skin lesions in dermoscopy images. Wherein each method have common three steps which are Preprocessing, Segmentation and Post-processing [13]. And the result depends on the metrics that is used to evaluate methods.

Lately [14] suggested a Multilevel Thresholding algorithm (MT) that iteratively divide the image histogram into several classes that identify the threshold value by the Otsu's method. Among the segmentation algorithms thresholding is said to be better because of its simple, fast and can get decent results in images that have a good contrast between the lesion and the skin. This technique in dermoscopy images sometimes fails because it does inconsistent result in some images there is smooth between the skin and lesion, and sometimes there is low contrast.

Researchers claim that region based methods is not easy in the situation of excessive types of colors with various skin types and textures in pigmented skin lesions, this demonstrates to over segmentation [5, 15].

According to their functionality segmentation of dermoscopy images it is divided into two techniques: supervised and unsupervised techniques. In supervised

segmentation technique, it requires user interaction while unsupervised technique does not need user interference and initialization. Furthermore unsupervised technique is ideal to make sure that the results are reproducible. Though in order to correct an improper segmentation results user intervention is still required [16].

There are many methods have been used in a segmentation dermoscopy image like region based method. [15], proposed the JSEG algorithm for segmentation of skin lesion. This algorithm consists of two parts: color quantization and spatial segmentation. Furthermore, [17] proposed statistical region merging (SRM) algorithm that is a new color image segmentation method based on region growing and region merging. This method is compared with (modified JSEG method, fuzzy c-means, mean shift clustering, and tumor extraction by dermatologist), the SRM got the best result.

For edge-based method, it is found in [20] that used geodesic active contour model or the geodesic edge tracing approach to the segment skin lesion. The snake (active contour) is the common segmentation method that uses in this area, especially in the medical image area. This method is based on distortion a curve towards the minimization of a given energy function.

A weak edge in some dermoscopy images makes a problem with edge-based approaches produce a smooth between the skin and lesions. For these problems are used contour that can solve the weak boundary to passing over it. Another problem there is a nice point (hair, skin line, air bubbles, blood vessels, etc.) that make the image appear less accuracy. That makes segmentation of skin lesion incorrectly. Furthermore, there are a wide number of parameters in this technique that impact the contour's attitude and implementation and it must be validated. [5, 21].

In order to discover the boundary of dermoscopy skin image (GVF) snakes is used [21]. For this study to segment the lesion image automatically, automatic snake initialization technique is used. The GVF is advantageous of being non sensitive to initialization and it has the ability to pass through concavities of the borders.

Six different techniques are recommended in the area of dermoscopy image segmentation [5], including both supervised and unsupervised segmentation tools: a) adaptive threshold, b) gradient vector flow (GVF), c) the level-set method, d) adaptive

snake (AS), e) expectation-maximization level set method (EM-LS), and f) fuzzy-based split and merge algorithm (FBSM). Silveira and her friends [5] found that the most appropriate segmentation results were found when using two supervised segmentation techniques, namely adaptive snake and the expectation-maximization level set tools. Also, they concluded that completely automatic techniques have somewhat poorer results. In our research, we compared three segmentation methods, including active contour modeling, the level set method, and fuzzy-clustering based on region growing (FCR), achieving high accuracy and high sensitivity of segmenting skin lesions using the fuzzy-clustering based on region growing method. We compared these three methods using accuracy, sensitivity, and specificity metrics.

CHAPTER 3

MATERIALS AND METHODS

The first step of digital segmentation is preprocessing. In the next chapter all the implemented segmentation methods in this thesis is discusses. In my work, I used 22 images of melanoma skin lesions obtained generously from the Pedro Hospital Hispano (HPH) database. The implementation of algorithms are performed with MATLAB® 2015. The MATLAB® built-in functions for image processing were the choice of the program.

3.1 PRE-PROCESSING

Pre-processing stage has three main steps;

a) converting the image from color (RGB) into grayscale
b) image filtering, and
c) detection of dark regions in the corners of the dermoscopy image.

In the following subsections the preprocessing steps are presented in details.

3.1.1 Image conversion from RGB to grayscale:

The first step is converting the RGB color image into a grayscale image [5, 13]. After that, the blue color channel from the image is chosen. It has been experimentally confirmed that the blue color channel in dermoscopy images presents the best contrast between lesions and the skin, thereby obtaining the best result for segmentation [5, 13].

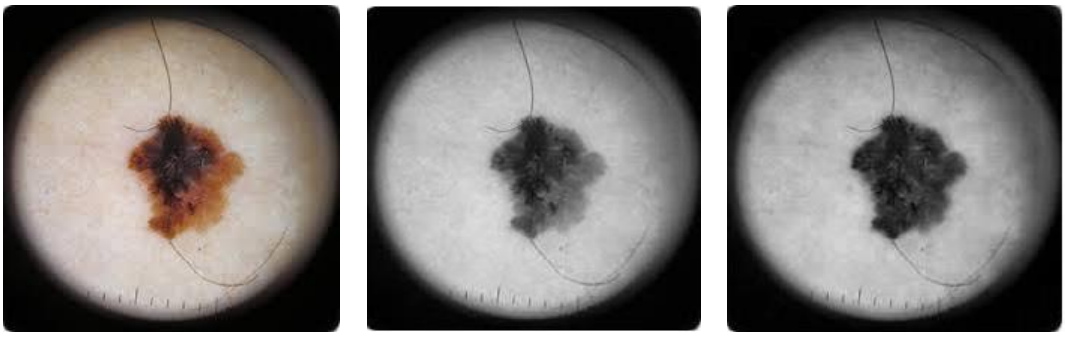

(a) Original Image **(b) Grayscale Image** **(c) Blue Channel Image**

Figure 3.1 Conversion of the image from RGB color space into grayscale.

Figure 3.1a, shows the original image of the skin lesion, Figure 3.1b shows the conversion of the original (RGB) image into grayscale, and Figure 3.1c shows the result of selecting the blue channel from the image.

3.1.2 Image filtering

For an accurate result of segmentation preprocessing, firstly, I smoothed the images using image filtering to remove some innate features of the image, such as dark hair, blood vessels, and air bubbles. We describe the filters in detail in Sections 3.1.2.1 and 3.1.2.2.

3.1.2.1 Hair removal

Dermoscopy images, mostly, have some hair textures and innate objects due to human nature. These affect segmentation, therefore I firstly removed these objects from the images. Abbas and Celebi, compared and analyzed different methods found in the literature on removing hairs from digital images [24]. The morphological close filtering is most accurate filtering among the list, this is the reason that I chose it. Morphological Close Filtering is used on grayscale images to remove the dark detail [25].

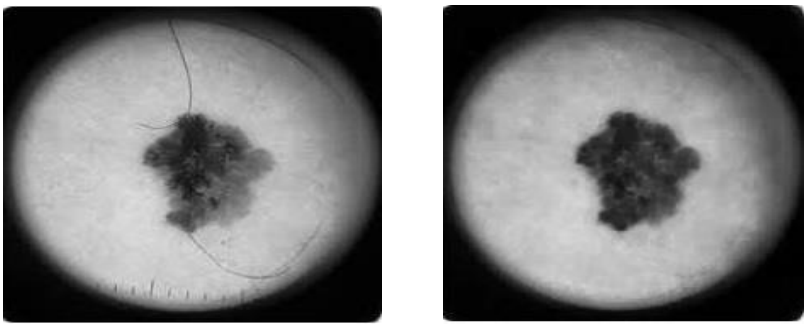

(a) **(b)**

Figure 3.2 (a) grayscale image; (b) the same image after using morphological close filtering.

Figure 3.2 shows an image with a dark hair or line, which is removed in Figure 3.2b using morphological close filtering.

3.1.2.2 Image smoothing

With the removal of hair from the dermoscopy image, some small, dark dots can be remain, one of the reasons is the hair may not be removed completely. To address this problem, I used a median filter to smooth the images. The median filter is a non-linear smoothing method that replaces the original gray-level pixels with the median pixels in a specified area:

$$y\,(i,j)\;=\;median\,\{\,x(m,n),(m,n)\;2\;z(\mathrm{i},\mathrm{j})\,\} \qquad (1)$$

In Equation 1, *x* is the input image, *y* is the output image, and *z* is an area centered at image coordinates (*i*, *j*) [19, 28].

This filter is useful to reduce noise. In our work, noise is indicated by dark points [19, 22, 26].

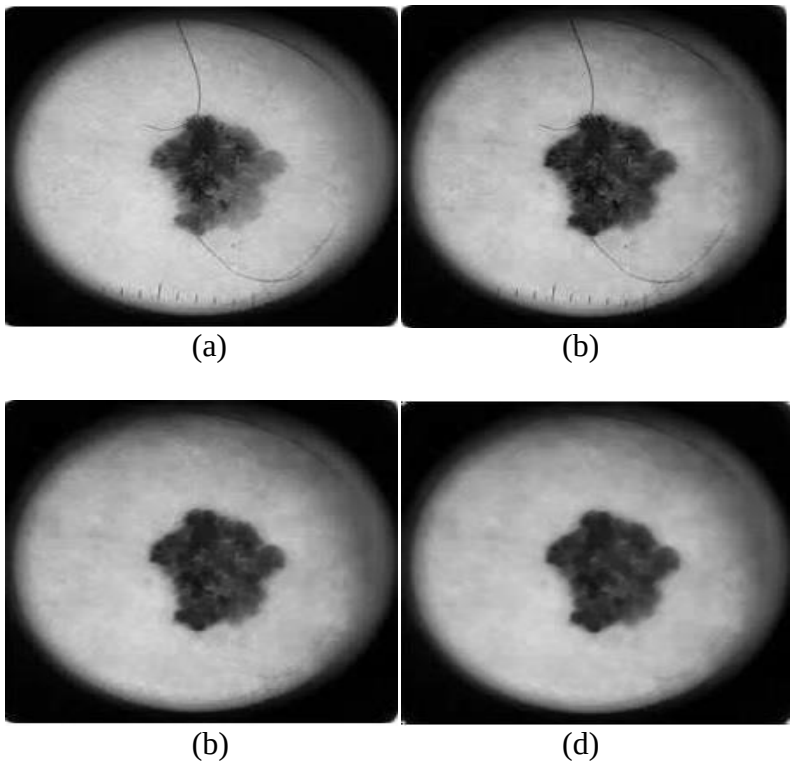

Figure 3.3 (a) grayscale image; (b) blue-channel image; (c) image after morphological close filtering; (d) image after using median filter.

Figure 3.3 shows the steps of the pre-processing process;

a) After converting the image from RGB to Grayscale.
b) Selecting the blue channel, which shows the image more clearly.
c) Removing hair from the image using morphological close filtering.
d) Using the median filter to reduce the noise.

3.1.3 Detection of dark regions in the corners of dermoscopy image

Most dermoscopy images have four dark regions, in grayscale these regions have the same intensity and will reduce the performance of segmentation. Using a binary mask for the four regions will remove this impact on the result of segmentation. First, I used Otsu's method for the image, after which the binary component is linked to the four corners of the image (see Figure 3.4).

Most dermoscopy segmentation methods use a binary mask for the dark corners because the pixels from the dark corners are not used; the binary mask is used to separate the image from the dark corner regions.

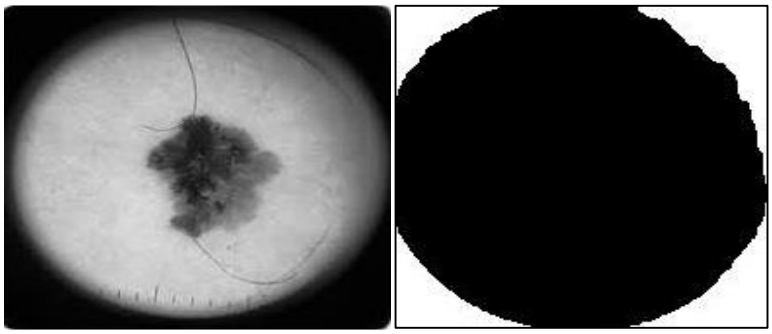

(a) (b)

Figure 3.4 (a) Original grayscale image; (b) binary mask of the dark regions at the four corners of the image.

Figure 3.4 shows the creation of a corner mask, both the grayscale original image, and the binary mask of the dark regions at the four corners of the image.

3.2 SEGMENTATION METHODS

Image segmentation is a procedure that separates an image into disjoint regions that are similar in some features, such as intensity, color, or texture. All of the regions that union must match to all images [22].

The primary aim of image segmentation is to divide an image into subregions that are disjoint in that they are optically different, but homogenous inside each region in terms of depth, motion, color, or gray level, with the goal to simplify the segmented image to make it more accurate and easier to analyze [27].

Many types of image segmentation methods are described in the literature. I implemented three of the most common image segmentation algorithms: active contour modeling, the level set method, and Fuzzy Clustering based on Region growing (FCR).

3.2.1 Active Contour

Active contours, also known as *snakes*, have been popular since 1987 and have been successfully applied to digital image segmentation [32]. Snake algorithms have been applied to the medical analysis of ultrasound images, among other medical applications.

Kass et al. were first to propose a model using snakes [30]. Since then, several new ideas have been proposed, such as different methods to minimize the total energy usage or new kinds of functional energy.

3.2.2 Level Set Method:

Level Set methodology has been proposed first time by Osher and Sethian [33]. This φ(x, y, t) is obtained for the development of the equation.

$$\frac{\partial \varphi}{\partial t} = \vec{F}|\nabla \varphi| + A.\nabla \varphi \qquad (2)$$

In Equation 2, the $\nabla \varphi$ is the gradient of evolution function and A is constant also F is Force of this model.

It is shown that initial condition φ (x, y, t = 0) = φ0 (x, y). Speed function depends on the expression of different applications. This may include many factors:

Front local specialties, such as in the normal direction and curvature, before the global properties, such as the shape and position and other independent operation based on external forces are spread in front of the display properties.

$$\frac{\partial \varphi}{\partial t} = \mu div(d_p|\nabla \phi|\delta_e) + \lambda \delta_e(\phi) div(g\frac{\nabla \phi}{|\nabla \phi|}) + \alpha g \delta_e(\phi) \qquad (3)$$

In Equation 3, the $\frac{\partial \varphi}{\partial t}$ is derivative of the level set function and α and μ is constant also δ is delta function and λ is constant.

This function "Distance Modulating Level Development Kit (MALSG)" called and allows iteration to be made with high time steps. This means that should the less iterations to reach the zero level edge. The segmentation of the reduction, however, in the number of iterations required for high-speed work is slow. To improve the segmentation speed, using the optimal number of iterations of the generated clusters to scan the whole picture instead of using a fuzzy clustering algorithm is projected to decrease and therefore increase speed.

Driven by an inner curvature on the right front first term evolution it is. The second term of information is represented by a deformation directed II. For a bright target object, I>λ indicates an expansion curve to move parts of the work object, and if I<λ indicates a contraction movement pieces for work outside of the curve object. Λ predefined threshold is lower depending on the intensity of the bright optical disc. The third term is the edge vector, which helps to stop the evolution of the curve in the optical disc limit. E is the parameters to control the balance of power.

Here it is driven by internal forces and external forces in front of the curvature k level set the edge vector g. Here, g is defined as an edge enhanced index and applied as follows by Gaussian smoothed image.

$$g(x,y)=\frac{1}{[1+|\nabla(G_{\sigma}(x,y)*I(x,y))|^{2}]} \tag{4}$$

Here, g is defined as an edge enhanced index and applied as follows by Gaussian smoothed image.

Level set free and deformation curve relatively early start allows you to have a uniform speed deformation zone. Then, the curve is the dominant deformation vector field edges to reduce edge spill neared the object boundary.

GVF (Gradient Vector Flow) is calculated as an image of the edge gradient map of a spatial diffusion, it is time-consuming calculations and GVF model map is not well defined edges. District-based model cloudy, with smooth borders to detect objects with highly effective gradient is poorly defined and the issue initially Chen and Vese [34] has been proposed. The new hybrid model is only as strong as the level set as the start curve, but at the same time using the GVF hybrid model of density information besides

the edges adds a more powerful force to stop functioning in the weak aside. Curves development of partial differential equations (PDE) by

$$\frac{\partial \varphi}{\partial t} = \mu div(d_p|\nabla \phi|\delta_e) - \frac{\partial \varepsilon_{ext}}{\partial \phi} \quad (5)$$

An S spatial parameter which sets the level function [0, 1] between the environmental point of t if [1, ∞) it indicates the time at the range. Curve development linked to these parameters, it is recognized.

$$\frac{\partial C(s,t)}{\partial t} = FN \quad (6)$$

Equation 6, is a velocity function that provides the motion control environment, equality, it is defined as the normal vector of the inherent vectors.

Here curve development (6) parameterized been set on level terms in formula If the conversion function in the dynamic environment C (s, t), time-dependent zero Level Set turns into function, i.e. Φ (x, y, t) becomes the function. Level set function negative values and positive values to zero level in the environment outside of it Assuming normal vector is defined as N = -∇Φ ∇Φ. Wherein ∇, the gradient operator.

The development curve formula (5) the equations of partial differential equations

When converted,

$$\frac{\partial \Phi}{\partial \Phi} = F/\nabla \Phi/ \quad (7)$$

is obtained to improved Level Set function. This model "Active Contour Models" or "Geometric Active Contour Model (GACM)" as it is called.

Re-Initialization:

Set the number of levels and the application of scientific and engineering problems despite the use of the method, due to irregularities in the application level set function to the development of. Traditional level set method, level set typical

irregularities in function occurs. This causes numerical error being and therefore impair the stability of the level set function. This numerical the name of the reinitialization improvements are made to solve the problem [35, 36].

This transaction marked improvement in function of the distance of the level set function periodically maintained by reinitialization to stop [36, 37]. Reinitialization evolution equation for steady state operation,

$$\frac{\partial C(\psi)}{\partial t} = sign\,(\Phi)(1 - /\nabla\psi/) \tag{8}$$

It is defined as. Φ function and the arrangements to be made here again the $sign\ (\Phi)$ function and is defined as (1.4) as in the formula It is described.

$$sign\,(x)\begin{cases} 1 & if\ f(x) > 0 \\ 0 & if\ f(x) = 0 \\ -1 & if\ f(x) < 0 \end{cases}$$

Ideally, a stable solution of this equation signed distance function. It reinitialization method commonly used in Level Set function [37, 38]. Another method used for reinitialization algorithm fast walking [35]. Although useful for numerical algorithm reinitialization improvement, zero level function can be set away from the expected location for the [35, 36]. It reinitialization reasons should be avoided wherever possible [35].

3.2.3 Segmentation Of Melanoma In Dermoscopy Images Based On Fuzzy Clustering Method And Image Region Growing:

There was a paper used an algorithm that integrated fuzzy-c-mean (FCM) and region growing techniques to automatically segment tumor images from patients with meningioma. The study used non-contrasted T1- and T2-weighted MR images from 29 patients with menigioma. After FCM clustering, 32 groups of images from each patient group were put through the region-growing procedure for pixels aggregation. Later, using knowledge-based information, the system selected tumor-containing images from these groups and merged them into one tumor image. An alternative semi-supervised method was added at this stage for comparison with the automatic method. Finally, the tumor image was optimized by a morphology operator. Results from automatic

segmentation were compared to the “ground truth” (GT) on a pixel level. Overall data were then evaluated using a quantified system [43].

In our method, we used fuzzy-c-mean clustering to segment skin cancer (melanoma). From three fuzzy clusters, we then calculated the standard deviation of each cluster, selecting the largest of them. After that, we used the image-region growing method for the selected cluster. In Subsections 3.2.3.1 and 3.2.3.2, we discuss fuzzy clustering and region growing.

3.2.3.1 Fuzzy clustering

In fuzzy clustering, each object belongs to a clustering class with different membership degrees. This algorithm is more useful in many situations than other clustering algorithms, in which an object is forced to completely belong to a single cluster class. After Zadeh’s introduction of fuzzy logic in 1965, a solution was suggested in which the similarity of each object to each class is illustrated by characterizing the similarity between an element and a group of functions by using membership values from 1 or 0. If the value is nearer to one, that means a greater similarity, while values near zero represent smaller similarities. Consequently, the fuzzy clustering problem is ideal for defining a characterization of this type [41]. The fuzzy clustering method has been broadly used in various fields, such as image processing, systems engineering, and parameter estimation.

3.2.3.2 Region growing

Region growing is a method that misuses spatial framework by collecting neighboring pixels together into big regions. The main principle in merging the region is similar. To recognize different objects there are some parameters as grayscale level, color and texture [19].

The procedure of region growing begins with a pixel or collection of pixels that is called as the seeds of a desired object. This process can be done manually in which user states an algorithm or it can be done automatically using seeds finding techniques. The following is scanning the neighbor pixels each time and put them in the growing region. In order to collect all homogenous pixels in the growing region, the process of finding non similar seeds is repeated until there is no pixels satisfy the homogeneity criteria

[22].

Region growing techniques usually get good results in segmentation that matches the edges of objects in an image that are visually seen. From this procedure, it is understood that areas inside an object grow and merge till their boundaries touch the edge of the object. However region growing algorithm is computationally more costly than the simpler methods, the techniques can be used to in applying numerous image parameters concurrently and directly in defining the last boundary location [19, 39].

One of the advantages of the region growing method is segmenting regions properly with similar properties and they are partitioned spatially. Furthermore, it produces connected regions. On the other hand the main problem of the region growing is the selecting of homogeneity criterion. In case of failure in choosing homogeneity criterion the region may spread out to neighboring regions or merge with areas that are not belonging to the desired object [23].

3.3 EVALUATION CRITERIA

There are different parameters that are used with the description of sensitivity, specificity and accuracy. The terms are True Positive (TP), True Negative (TN), False Negative (FN), and False Positive (FP).

In case of identifying a disease in a patient if the diagnostic analysis also shows the presence of the disease, then the result of the test is said to be (TP).

In case of identifying an absence of a disease in a patient if the diagnostic analysis also shows the absence of the disease, then the result of the test is said to be (TN).

TP and TN indicate a reliable result between the diagnostic analysis and the proved disease.

Though every diagnostic investigation are not correct, so when the test result shows a disease that is not existed in the patient the test result is considered as FP. And if the test fails to indicate the disease that exists in the patient for sure, the result is FN.

Both of FP and FN show that the diagnostic result conflict with the real situation.

3.3.1 Sensitivity

Sensitivity is a measure which indicates the proportion of the true positive samples from diagnostic set, correctly identified as positive samples and can be expressed as follow:

Sensitivity = $\frac{TP}{TP+FN}$ this means (Number of true positive assessment)/ (Number of all positive assessment)

The numerical values of sensitivity indicate the likelihood of a medical test represents patients with the disease so when the sensitivity value is high, it is difficult to extract information form a FP test result. For instance, assume a sensitivity value is 99%, this means that when a patient who for sure has a disease makes a diagnostic investigation the probability of that patient to be stated as positive is 99%. High sensitivity supposed to detect all positive situations without missing any case. Hence a test that has high sensitivity is usually to display a disease.

3.3.2 Specificity

Specificity is a measure of the ability of the classifier to accurately identify the proportion of negative samples correctly identified from the negative samples and can be expressed as follows:

Specificity = $\frac{TN}{TN+FP}$ it means (Number of true negative assessment)/ (Number of all negative assessment)

The numerical values of specificity indicate the likelihood of a medical test a specific disease exclusive of providing FP results. For instance, assume the specificity value of an investigation is 99%, it shows that a patient's lack of a particular disease who make a medical test has a probability of 99% of being negatively classified.

3.3.3 Accuracy

Accuracy is defined as the proportion of the samples correctly classified out of the

total number of samples and can be defined as follows:

Accuracy $=\frac{(TN+TP)}{(TN+TP+FN+FP)}$ it means (Number of correct assessments)/Number of all assessments).

A medical test might be specific, but not sensitive or vice versa. These factors are both equivalently vital for a good test result must have high value of sensitivity and specificity such as a pregnancy test. When a woman has a positive result in pregnancy test it is roughly defined that woman is pregnant. Also a negative test result shows the lack of pregnancy in that woman.

Beside the mathematical equation shown above if the prevalence is known, it is possible to determine accuracy from sensitivity and specificity. Prevalence is the likelihood of existing a disease at a certain time:

$$Accuracy = (sensitivity)(prevalence) + (specificity)(1 - prevalence) \quad (9)$$

The numerical value of accuracy indicates the quantity of both true positive and true negative results in a particular population. In most of the situations an accuracy of 99% times the test result is accurate, regardless positive or negative. But it is important to declare that in case of high ratio of sensitivity and specificity it does not mean that the accuracy is high as well. Together with specificity and sensitivity, accuracy is also decided by how common the disease is in the particular population. An analysis of uncommon situations in a selected population can have a result of high sensitivity and specificity but low accuracy. Thus, it must be very careful whilst interpret accuracy result [42].

CHAPTER 4

RESULTS

In this chapter, experimental results are presented. The result are classification of three methods (active contour, level-set method, and fuzzy clustering based on region growing) by the evaluation of the performance of the segmentation methods.

4.1 ACTIVE CONTOUR

The concept is based on the description of the object contour by a parametric curve. Their form is corrected as a function of so-called internal and external energies after an often manual initialization. The external energy, calculated in this case from the image content in relation to the position of the contour. Often this is a form of gradient is used (GVF). The internal energies are calculated only from the shape of the contour. By a minimization algorithm, the shape of the contour is calculated, in which the sum of all energies reaches a minimum. Instead of the minimization can actually be carried out very often changed and then considered that form as a result of the shape of the snake, in which the sum of the energies is minimal [31].

In this study, we used 120 iterations for the convergence of the algorithm.

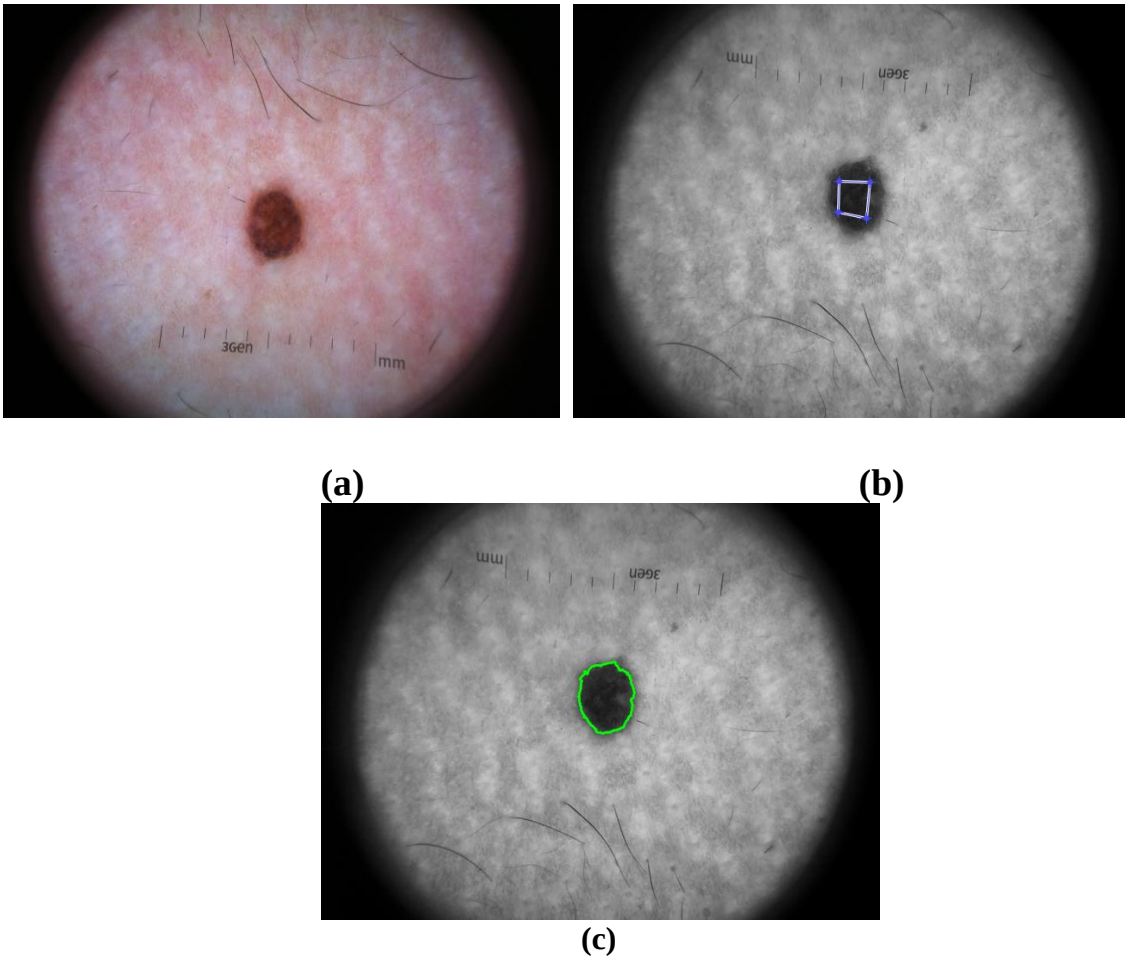

Figure 4.1 a) Original skin image from dermoscopy; b) initial contour; c) segmented skin lesion.

Figure 4.1 shows the segmentation of a skin lesion imaged by dermoscopy using the active contour model over 120 iterations for the convergence of the algorithm.

We calculated the area, perimeter, and centroid of the segmented object; these results are shown in Table 4.1 In this table, the area is in number of pixels in the area segmented in the image. Also, perimeter values represent the perimeter of a segmented cancer object. The centroid of each object in the images are represented by X and Y coordinates.

Table 4.1. Simulation results, active contour method.

Image	Area	Perimeter	Centroid (X)	Centroid (Y)
1	7724	476.051	107.0647	76.20469
2	5813	402.041	87.37296	77.16945
3	3111	366.578	129.3041	84.69142
4	2603	283.686	99.61468	68.94737
5	3616	334.375	86.53595	76.5141
6	3460	271.24	105.0312	76.19711
7	6967	459.965	48.92665	53.06689
8	6451	363.502	91.83243	72.4652
9	4993	302.799	72.26517	65.18486
10	2443	196.964	94.02374	69.66598
11	2581	215.498	61.86478	68.06548
12	3249	217.003	103.7101	88.67775
13	4028	255.832	104.7438	86.73312
14	6883	521.631	73.44167	68.91385
15	2331	224.379	99.77864	92.17932
16	4619	332.035	100.9502	75.60749
17	6892	451.581	104.613	66.98476
18	7646	459.809	98.79689	74.57036
19	11489	568.398	78.88694	68.95187
20	3240	235.809	87.04691	85.04599
21	2264	218.187	92.4894	56.93993
22	3132	277.855	108.8758	84.23276

4.2 LEVEL SET METHOD

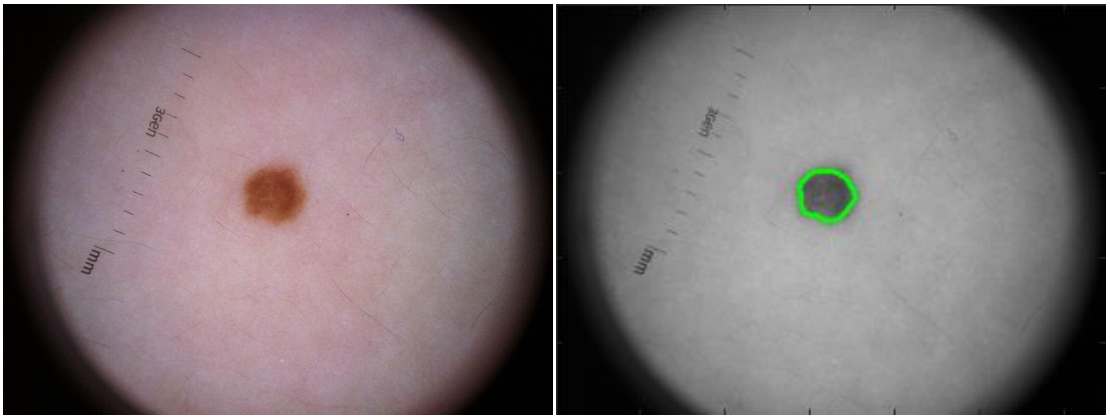

(a) **(b)**

Figure 4.2 a) original; and b) segmented image.

Figure 4.2 shows the segmentation of a skin lesion using the level set method over 40 iterations.

We calculated the area, perimeter, and centroid of the segmented object; these results are shown in Table 4.2. In this table, the area is in number of pixels in the area segmented in the image. Also, perimeter values represent the perimeter of a segmented cancer object. The centroid of each object in the images are represented by X and Y coordinates.

Table 4.2 Simulation results, level set method.

Image	Area	Perimeter	Centroid (X)	Centroid (Y)
1	6216	306.213	108.5301	77.20849
2	3556	226.313	195.722	126.820
3	5962	297.703	86.421	78.75981
4	963	108.021	44.054	39.521
5	2481	231.318	128.705	82.27731
6	2923	201.318	99.424	92.3143
7	2457	209.038	99.99308	70.43956
8	4703	257.021	72.7324	66.8043
9	3505	212.718	88.83823	78.00285
10	12075	410.514	90.2034	75.20476
11	2771	226.776	106.9329	81.2389
12	2710	196.0543	93.9026	70.6043
13	3233	233.898	59.31704	68.97742
14	3618	253.843	65.0043	64.5093
15	6308	289.466	91.65758	75.6598
16	3501	213.0	103.1493	89.2304
17	4587	254.432	74.35165	66.35797
18	6737	328.143	72.2847	71.2920
19	2452	192.134	93.9894	70.93148
20	11898	556.832	93.0213	71. 8043
21	2965	213.703	64.6027	68.02361
22	2361	182.214	99.4325	93.3403

4.3 SEGMENTATION OF MELANOMA IN DERMOSCOPY IMAGES FUZZY CLUSTERING METHOD BASED ON IMAGE REGION GROWING (FCR)

In this study, I used three clusters for fuzzy clustering and also to grow the region. The intensity threshold was set at 0.49. These values were derived experimentally, as shown in Table 4.3.

Table 4.3. Intensity threshold.

parameters	t	Number of clusters
values	0.49	3

We determined that three clusters was enough, because with more than three clusters, we obtained a poor result. In the following figures, we show the results of using two, three, four, five, and six clusters.

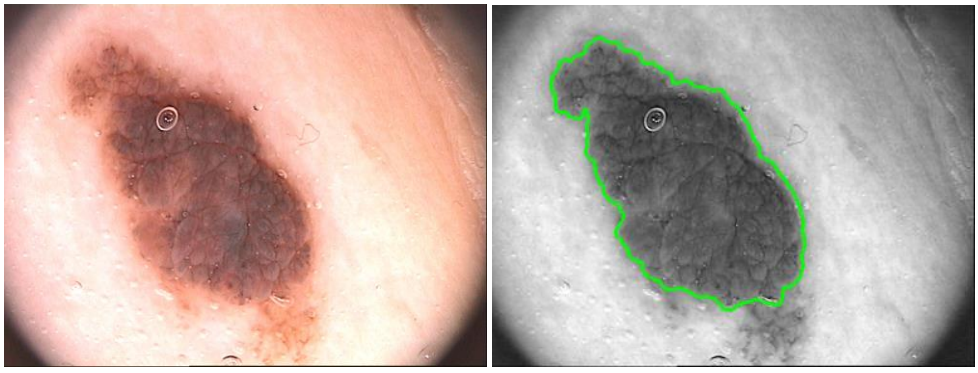

(a) (b)

Figure 4.3 a) Original image; b) image after fuzzy-clustering mean algorithm; c) results of simulation; d) segmenting cancer.

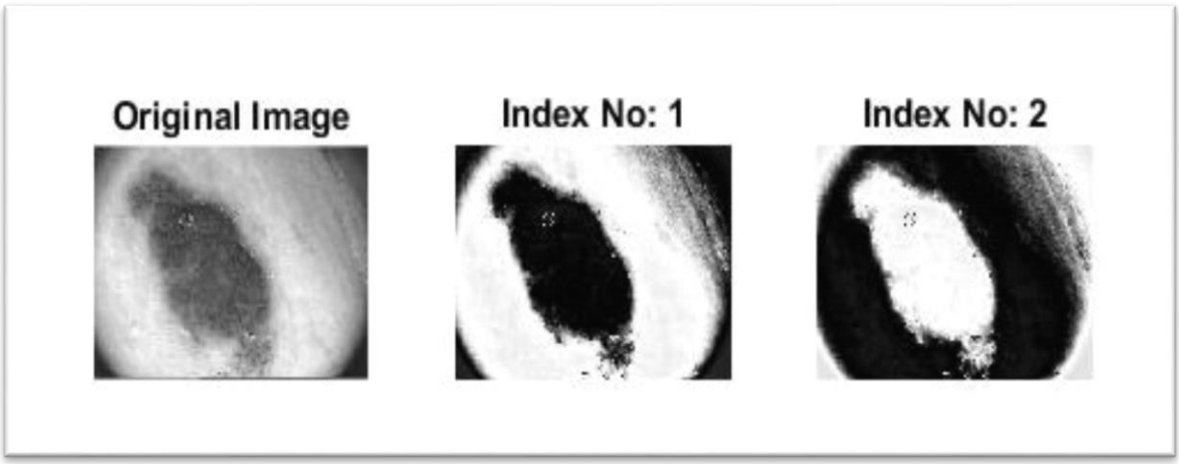

Figure 4.4 Number of cluster =2.

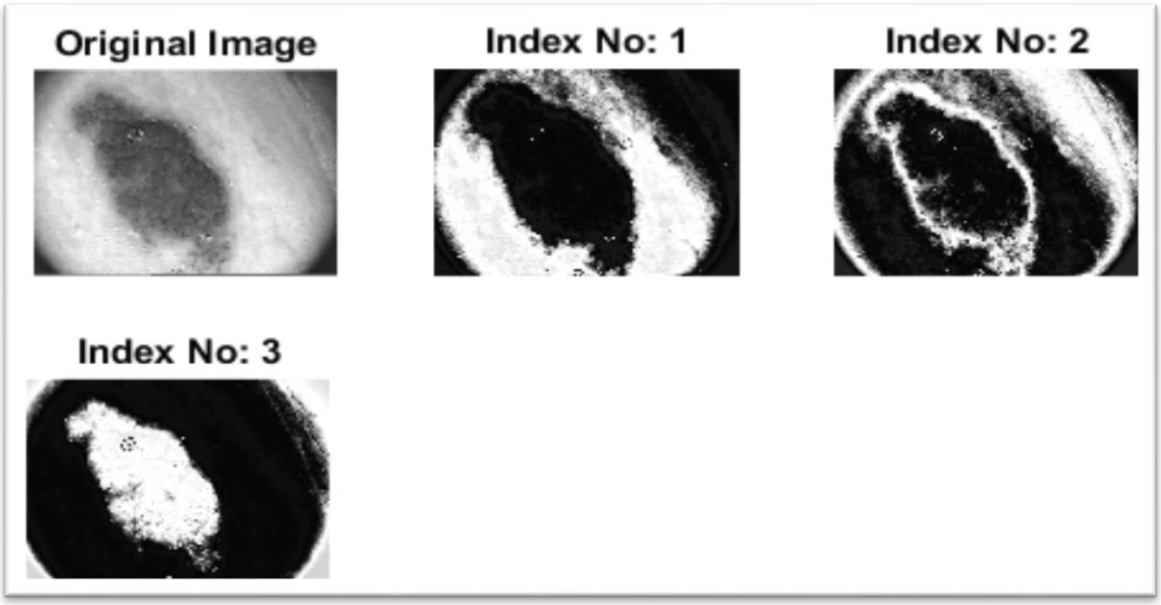

Figure 4.5 Number of cluster =3.

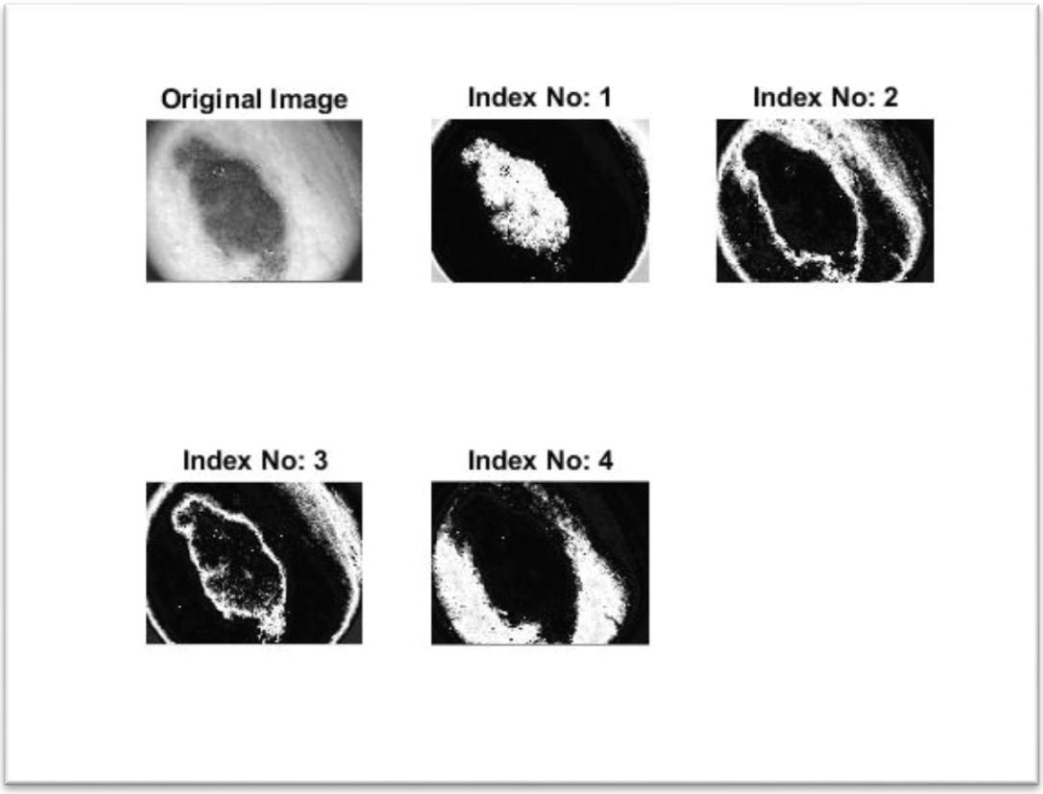

Figure 4.6 Number of cluster = 4.

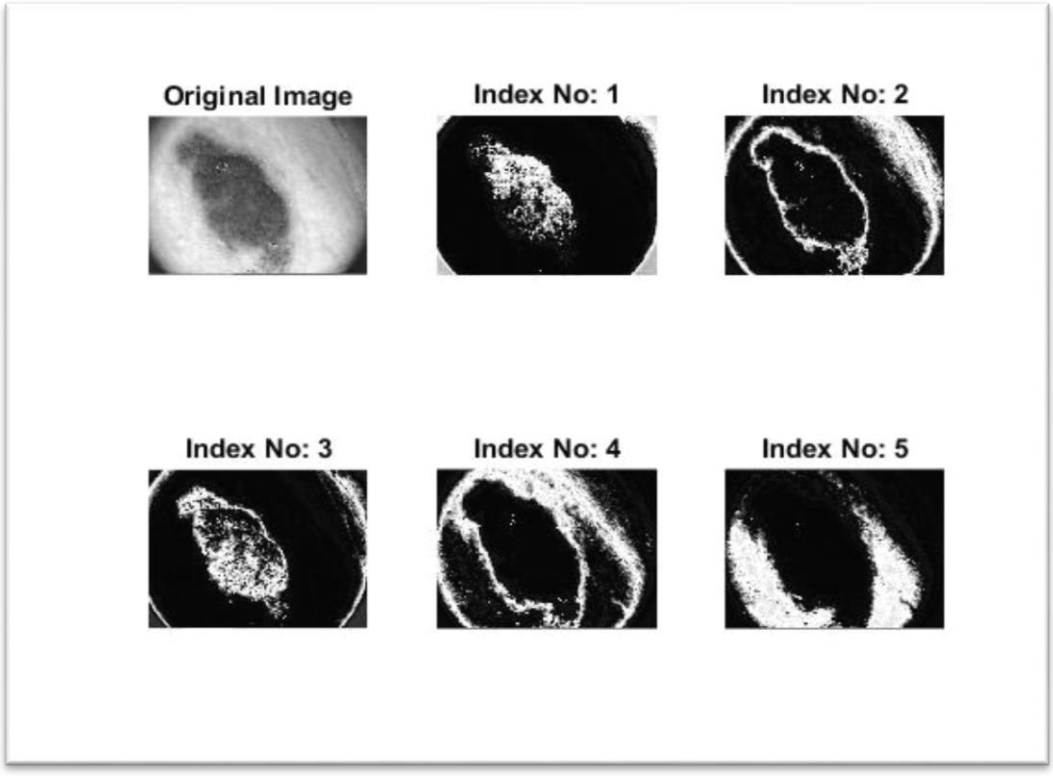

Figure 4.7 Number of cluster =5.

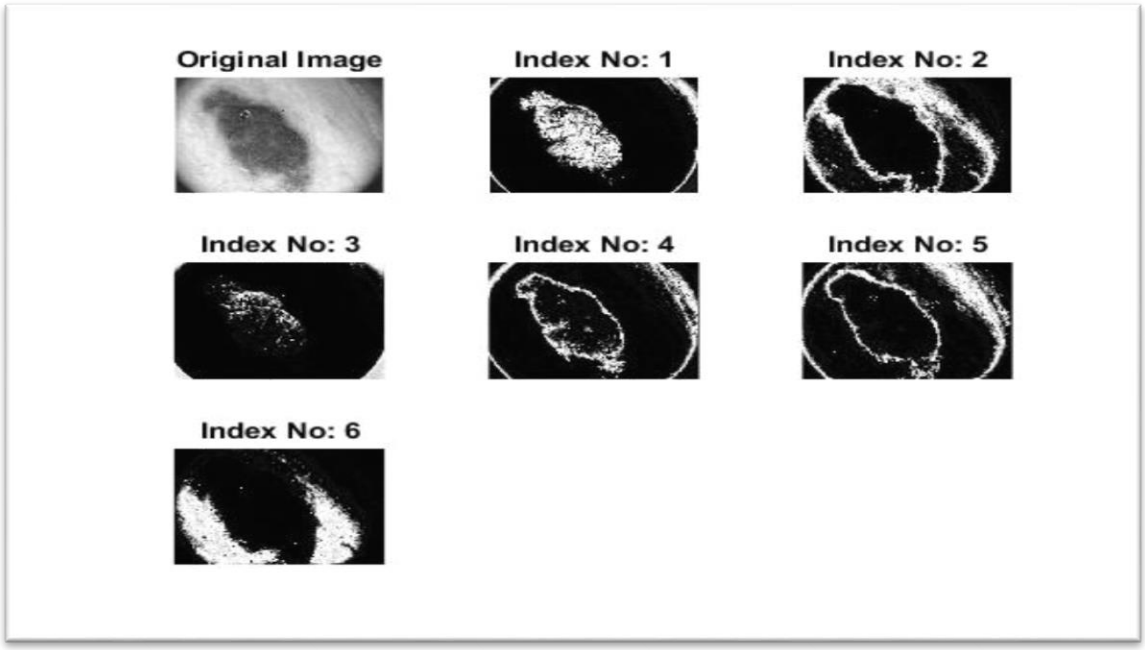

Figure 4.8 Number of cluster =6.

As may be seen in these results, there is no need for more than three clusters.

(a)

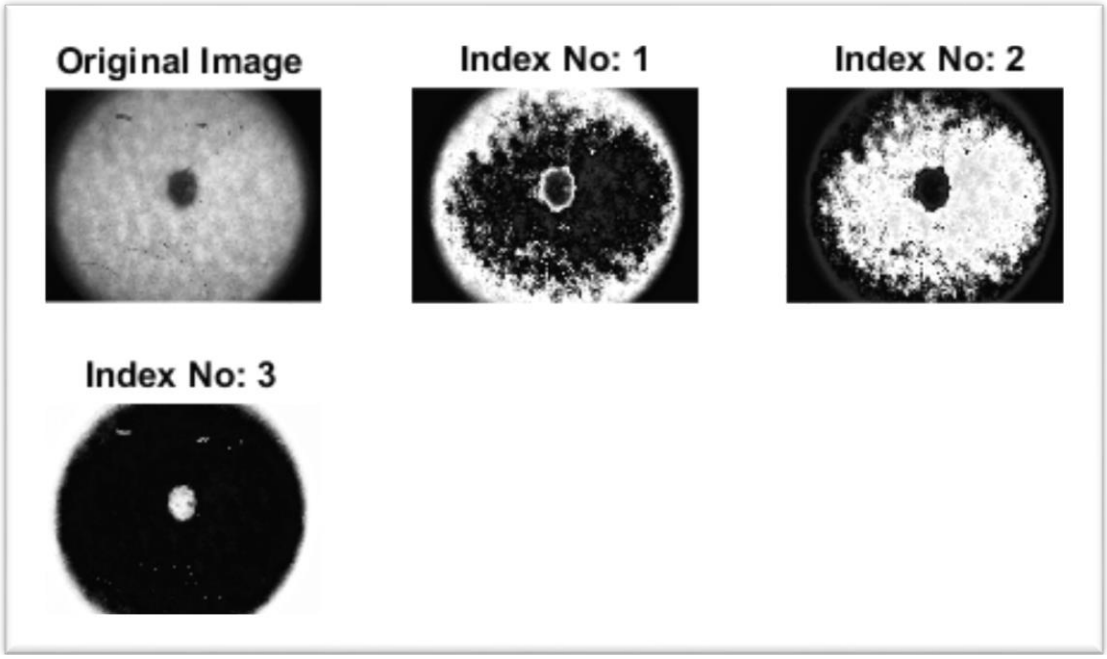

(b)

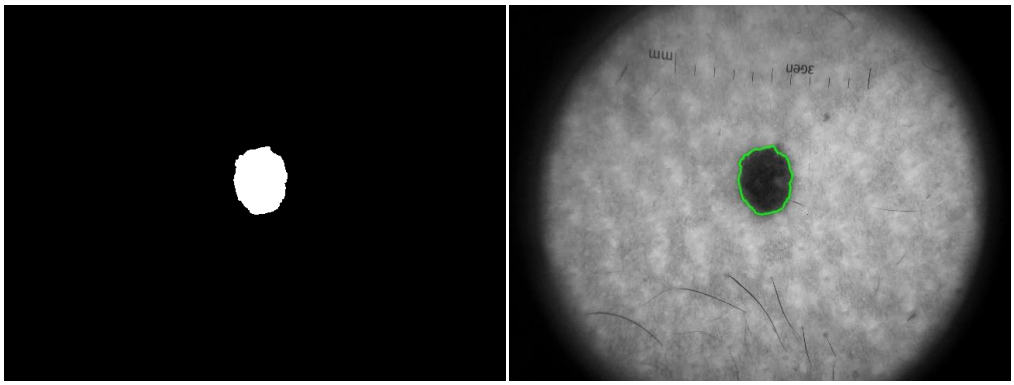

(c) (d)

Figure 4.9 a) Original image; b) segmented cancer; c) result of fuzzy-clustering mean algorithm.

(a) **(b)**

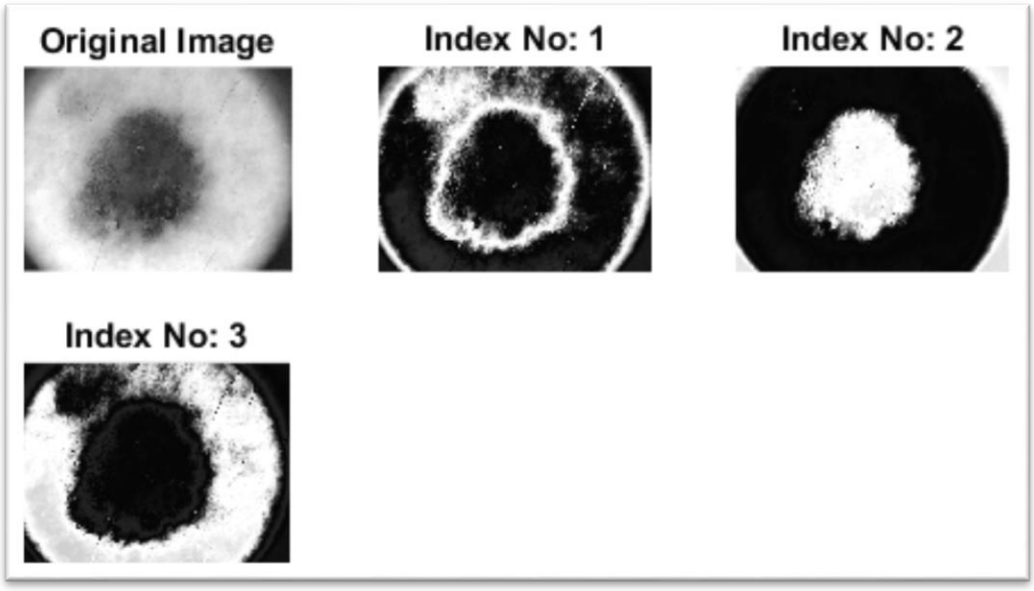

(c)

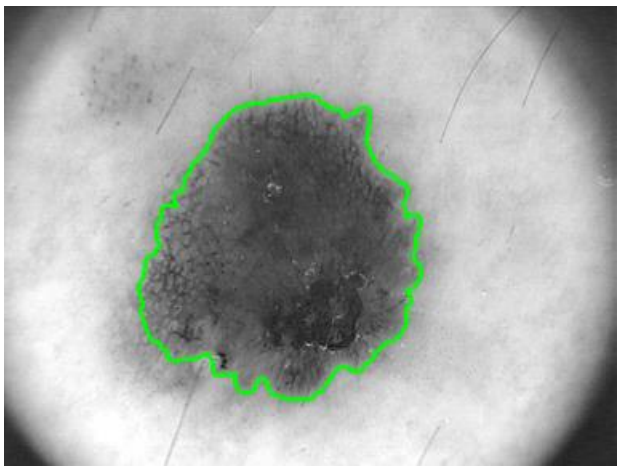

(d)

Figure 4.10 a) Original image; b) result of simulation; c) result of fuzzy-clustering mean algorithm; d) segmented Lesion.

We calculated the area, perimeter, and centroid of the segmented object; these results are shown in Table 4.4. In this table, the area is in number of pixels in the area segmented in the image. Also, perimeter values represent the perimeter of a segmented cancer object. The centroid of each object in the images are represented by X and Y coordinates.

Table 4.4 Simulation results, FCR.

Image	Area	Perimeter	Centroid (X)	Centroid (Y)
1	33604	884.218	213.4855	153.2312
2	24355	664.19	175.0958	153.4601
3	13692	584.35	257.8634	168.4694
4	11999	533.546	199.1358	137.4722
5	14627	523.24	167.6111	150.6204
6	15408	477.556	210.1937	151.3294
7	28430	900.889	97.97622	106.96
8	27529	670.014	183.362	145.0463
9	21988	575.798	144.3662	130.2754
10	11186	412.652	187.4136	139.3082
11	11854	414.314	123.9106	136.0914
12	14563	456.906	206.9107	176.7432
13	18023	514.508	209.1787	173.4053
14	30339	787.312	146.4895	136.8762
15	10867	433.98	199.579	184.6637
16	20167	619.16	202.0086	150.432
17	29877	717.946	208.6524	133.3929
18	29319	761.91	200.3186	153.8177
19	49023	899.32	157.263	137.6751
20	14824	484.042	172.796	169.362
21	10082	403.57	185.1071	113.8908
22	15010	639.318	216.6837	164.9803

4.4 EVALUATION CRITERIA

In Table 4.5, we calculate the accuracy, sensitivity, and specificity for active contour models.

Table 4.5 Sensitivity, specificity, and accuracy for active-contour model.

Image	Accuracy	Specificity	Sensitivity
1	0.975842	0.978841	0.972843
2	0.982416	0.975715	0.989118
3	0.884747	0.99619	0.773304
4	0.908253	0.999959	0.816548
5	0.969128	0.974805	0.96345
6	0.989818	0.980967	0.99867
7	0.958248	0.931158	0.985339
8	0.981017	0.986678	0.975355
9	0.989583	0.982425	0.996742
10	0.982554	0.998172	0.966935
11	0.980047	0.995864	0.964231
12	0.983526	0.995755	0.971296
13	0.992432	0.984864	1
14	0.951686	0.994743	0.908629
15	0.96834	0.993489	0.943192
16	0.966605	0.996239	0.936972
17	0.977956	0.959867	0.996046
18	0.938405	0.975834	0.900976
19	0.982676	0.984768	0.980583
20	0.990736	0.985613	0.995859
21	0.987942	0.991674	0.984211
22	0.981413	0.962826	1

Table 4.6 Sensitivity, specificity, and accuracy for the level-set method.

Image	Accuracy	Specificity	Sensitivity
1	0.909615	0.997744	0.821486
2	0.981425	0.969979	0.992871
3	0.805007	0.999026	0.610987
4	0.879642	0.999754	0.759529
5	0.991228	0.98406	0.998397
6	0.904601	0.987785	0.821417
7	0.792466	0.999955	0.584977
8	0.969476	0.986819	0.952133
9	0.972615	0.991495	0.953736
10	0.981731	0.997735	0.965726
11	0.991185	0.985063	0.997308
12	0.987848	0.998228	0.977469
13	0.981069	0.997814	0.964325
14	0.861988	0.990874	0.733102
15	0.846901	0.999526	0.694276
16	0.882027	0.999481	0.764573
17	0.953549	0.996061	0.911038
18	0.836939	0.99586	0.678017
19	0.946954	0.995693	0.898215
20	0.983982	0.99557	0.972395
21	0.918122	0.999881	0.836364
22	0.911852	0.998692	0.825011

Table 4.7 Sensitivity, specificity, and accuracy for FCR.

Image	Accuracy	Specificity	Sensitivity
1	0.971037	0.951466	0.990608
2	0.978406	0.9639	0.992913
3	0.992068	0.996036	0.828101
4	0.947457	0.995822	0.899093
5	0.92538	0.963766	0.886995
6	0.982445	0.964891	1
7	0.950211	0.922532	0.97789
8	0.979424	0.970233	0.988616
9	0.980435	0.960869	1
10	0.993553	0.987409	0.999698
11	0.990822	0.984916	0.996728
12	0.990654	0.98316	0.998148
13	0.982272	0.964544	1
14	0.965321	0.977639	0.953002
15	0.989038	0.983275	0.9948
16	0.978841	0.9859	0.971782
17	0.967323	0.934646	1
18	0.992641	0.972431	0.852851
19	0.972747	0.949131	0.996364
20	0.983468	0.966937	1
21	0.991278	0.982796	0.99976
22	0.969536	0.939073	1

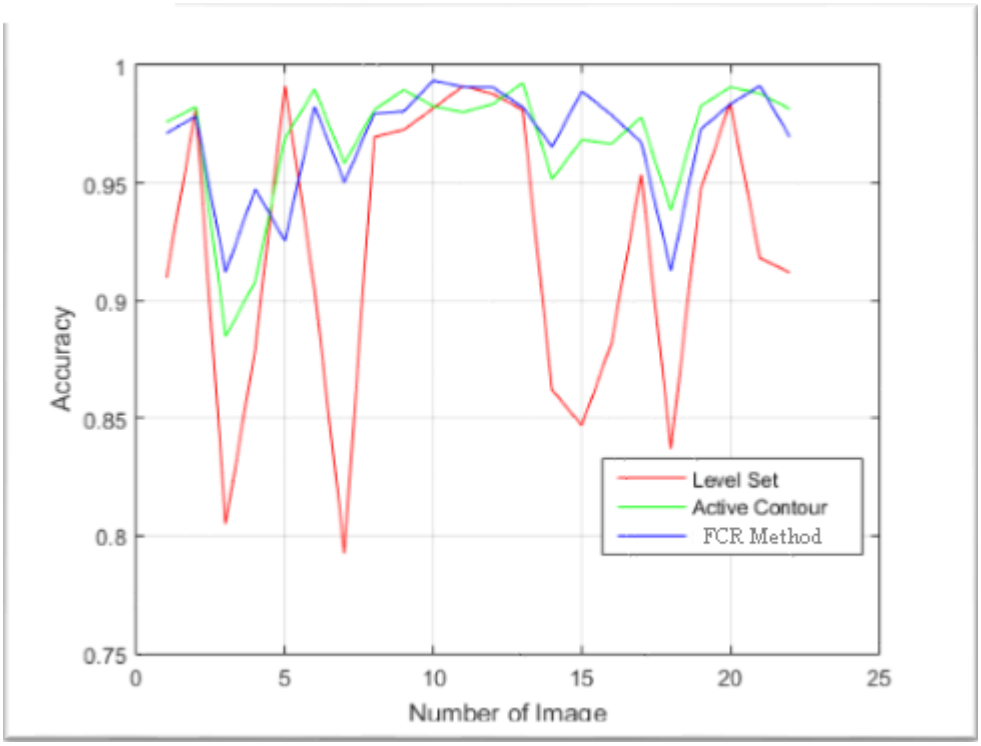

Figure 4.11 Calculating accuracy for the level-set method, active contour, and fuzzy-clustering based on region growing.

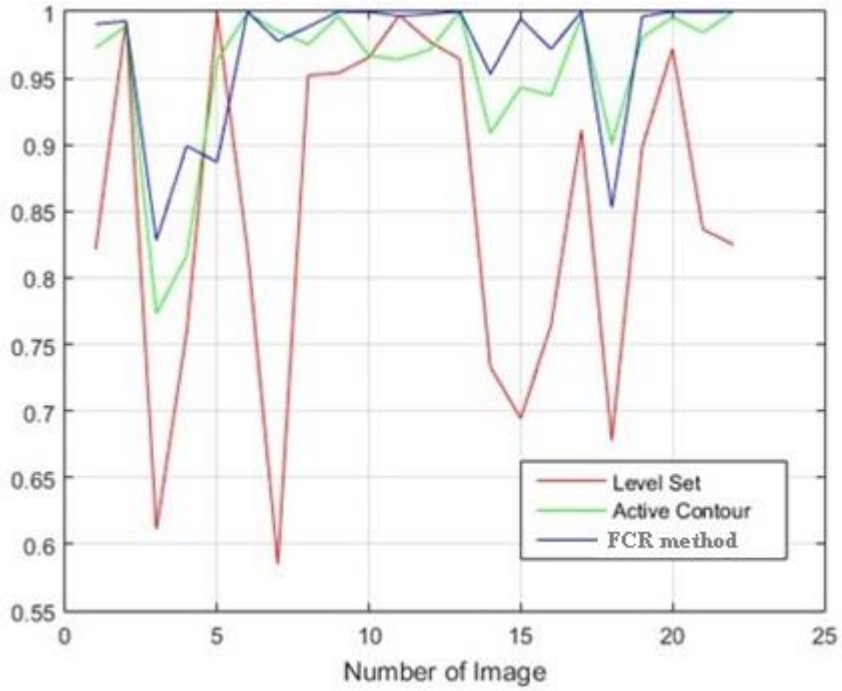

Figure 4.12 Calculating sensitivity for the level-set method, active contour, and fuzzy-clustering based on region growing.

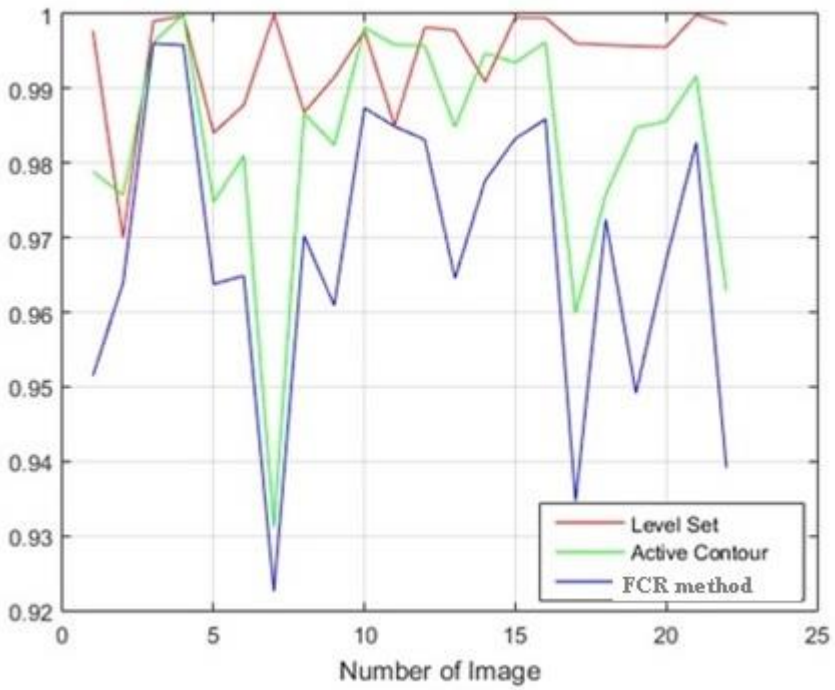

Figure 4.13 Calculating specificity for the level-set method, active contour, and fuzzy-clustering based on region growing.

Table 4.8 The average calculated criteria for each segmentation method applied to 22 images. The values in bold correspond to the best performance on each metric.

Method	Accuracy (%)	Specificity (%)	Sensitivity (%)
Active Contour	96.2	98.30	95.54
Level Set Method	92.22	**99.39**	85.06
FCR	**97.6**	96.82	**96.94**

CHAPTER 5

DISCUSSION AND CONCLUSION

5.1 DISCUSSION

Skin cancer is among the most common types of human cancer and Melanoma is the most dangerous of the skin cancers [1]. Because of the increasing rate of skin cancer, it is recognized both nationally and internationally. For medical diagnosis and analysis, the extraction of Melanoma from images of skin lesion plays an important role. Early detection will save many people's lives, and classical medicine techniques are not enough to detect this dangerous disease. Current advancement in technology has a role to play in this detection. One way to clearly detect or show the image of cancer is segmentation. Several segmentation algorithms have been suggested to apply to this problem, comprising four major types of method: thresholding, edge/contour-based, region-based, and clustering based methods. Many researchers have been working on computer-vision approaches to skin-cancer detection. To segment skin lesions in an input image, existing systems use manual, semi-automatic, or fully automatic methods.

Selveria et al. recommended six different techniques for dermoscopic image segmentation [5], including adaptive thresholding, gradient vector flow (GVF), the level-set method, adaptive snake (AS), and the expectation-maximization level-set (EM-LS) method. Applied to 100 dermoscopy images, they found that the most appropriate segmentation used two supervised segmentation techniques, namely adaptive snake and the expectation-maximization level-set tools. Also, they concluded that completely automatic techniques achieve somewhat poorer results. These methods were evaluated based on four metrics: Hammude Distance, True Detection Rate, False Positive Rate, and Hausdorff Distance.

Following these studies, my work to detect skin cancer is proposed. Three different methods; active contour, the level-set method, and a new proposal within this work named fuzzy-clustering method based on region growing are compared. These methods have never before been compared together in one study. We implemented our method on 22 images that we obtained from Pedro Hospital Hispano (HPH). We selected images randomly and ground-truth images were available in the database. We used three different metrics to compare these three methods: accuracy, sensitivity, and specificity. The best method was our proposed method of fuzzy clustering based on a region growing method, which has high accuracy (97.6%) and high sensitivity (96.4%). Its specificity was (96.82%). The active contour model had accuracy of 96.92%, sensitivity of 95.54%, and specificity of 98.30%. The level-set method had accuracy of 92.22%, sensitivity of 85.06%, and specificity of 99.39%. According to these results, our proposed method obtained the best result in terms of accuracy and sensitivity. Regarding specificity, the best result was obtained from the level-set method. The fastest execution time was with the active contour method.

We used an active contour model to segment skin lesions, active contour is one of the segmentation methods used commonly to segment and analyze medical images in the literature. The biggest advantages of active contour are that it partitions an image into sub-regions with continuous boundaries [40]. As a result, our FCR method is better than the other methods; it is also more robust than the other methods, because our method alone uses fuzzy clustering to find the object. A future work might increase the number of sample images and use different processing algorithms to reach a better classification.

5.2 CONCLUSION

Melanoma skin cancer is the most widely diagnosed type of cancer. As the number of cases grows each year, effective, quick, and early detection of melanoma is very important. If skin cancer is detected in early stages, it may be treated easily. The removal of skin-cancer lesions at last stages is expensive, while in early stages lesions are easy and economical to treat.

To achieve an active way to detect malignant melanoma early without doing unnecessary skin biopsies, digital image segmentation for skin lesions has been investigated. Among imaging techniques, dermoscopy is the most suitable for melanoma diagnosis. Image segmentation is very important in digital image processing and allows automatic discovery of the details of objects in important areas. This capability has an important role to play in solving many difficult problems, particularly problems related to many chronic diseases, such as skin cancer.

In this study, we used three segmentation methods to detect melanoma skin cancer: a) active contour, b) level-set method, and c) fuzzy-clustering based on region growing. After simulation, and after evaluating each method in terms of accuracy, sensitivity, and specificity, we obtained the best result from our proposed method, fuzzy-clustering based on region growing, as it demonstrated both high accuracy and high sensitivity. To evaluate these methods, we obtained 22 images from Pedro Hospital Hispano (PHP). All images were evaluated by medical expert. In this work, we proposed a new method and compared it with two other methods that have never before been compared together in any study.

REFERENCES

[1] Kopf, A. W., T. G. Salopek, et al., “Techniques of cutaneous examination for the detection of skin cancer”, PubMed.gov, 75(2 Suppl):684-90, 15 jan 1995.

[2] MacKie, R. M. Skin Cancer, 2nd edition, UK, 1996.

[3] Washington, C. M., and D. T. Leaver, Principles and Practice of Radiation Therapy, U.S, 2015.

[4] Deserno, T. M. Biomedical Image Processing (Biological and Medical Physics, Biomedical Engineering), Germany, 2010.

[5] Silveira, M., J. C. Nascimento, et al., "Comparison of Segmentation Methods for Melanoma Diagnosis in Dermoscopy Images", IEEE Journal Of Selected Topics In Signal Processing, Vol. 3, NO. 1, February 2009.

[6] Abdulbaki, A. S. Skin Cancer Image Segmentation & Detection by using Unsupervised Neural Networks (UNN), M.S. Thesis, Anbar University, 2012.

[7] El-Zaart, A. "Skin Images Segmentation", Journal of Computer Science 6 (2): 217-223, ISSN 1549-3636, 2010.

[8] Kanitakis, J., "Anatomy, histology and immune histochemistry of normal human skin", pubMed.gov, 12(4):390-9; quiz 400-1, Aug 2002.

[9] Wiles, M. R., J. Williams, et al., Essentials of Dermatology for Chiropractors, USA 2011.

[10] National cancer institute, N. C. I., what you need to know about melanoma and other skin cancer, Spain, 2010.

[11] Benvenuto, A. C., S. W. Dusza, et al., "Differences between polarized light dermoscopy and immersion contact dermoscopy for the evaluation of skin lesions". Archives of dermatology, Vol 143, No.3, March 2007.

[12] Sadeghi, M. Towards Prevention And Early Diagnosis Of Skin Cancer: Computer-Aided Analysis Of Dermoscopy Images, Ph.D. Thesis, Simon Fraser University, 2012.

[13] Celebi, M. E., G. Schaefer, et al., "Lesion border detection in dermoscopy images," Computerized Medical Imaging and Graphics, vol. 33, pp. 148–153, March 2009.

[14] Humayun, J., A. S. Malik, et al., "Multilevel thresholding for segmentation of pigmented skin lesions," Proceedings of IEEE International Conference on Imaging Systems and Techniques, pp. 310–314, May 2011.

[15] Celebi, M. E., Y. A. Aslandogan, et al., "Unsupervised border detection of skin lesion images," Proceedings of the International Conference on Information Technology: Coding and Computing, vol. 2, pp. 123–128, April 2005.

[16] Sharma, N. and L. M. Aggarwal, "Automated medical image segmentation techniques," Journal of Medical Physics, vol. 35, pp. 3–14, January 2010.

[17] Celebi, M. E., H. A. Kingravi, et al., "Border detection in dermoscopy images using statistical region merging," Skin Research and Technology, vol. 14, pp. 347–353, August 2008.

[18] Wang, H., X. Chen, et al., "Watershed segmentation of dermoscopy images using a watershed technique," Skin Research and Technology, vol. 16, pp. 378–384, August 2010.

[19] Wu, Q., F. Merchant, et al., Microscope Image Processing. Academic Press,1 ed., USA, April 2008.

[20] Chung, D. H. and G. Sapiro, "Segmenting skin lesions with partial-differential equationsbased image processing algorithms," IEEE Transactions on Medical Imaging, vol. 19, pp. 763–767, July 2000.

[21] Erkol, B., R. H. Moss, et al., "Automatic lesion boundary detection in dermoscopy images using gradient vector flow snakes," Skin Research and Technology, vol. 11, pp. 17–26, February 2005.

[22] Gonzalez, R. C. and R. E. Woods, Digital image processing. Upper Saddle River: Prentice Hal, 2 ed., 2002.

[23] Bankman, I. N., Handbook of medical imaging: processing and analysis. Academic Press, 1 ed., 2000.

[24] Abbas, Q., M. E. Celebi, et al., "Hair removal methods: A comparative study for dermoscopy images," Biomedical Signal Processing and Control, vol. 6, no. 4, pp. 395–404, 2011.

[25] Barata, C., J. S. Marques, et al., "Detecting the pigment network in dermoscopy images: a directional approach," International Conference of the IEEE Engineering in Medicine and Biology Society, pp. 5120–5123, 2011.

[26] Sonka, M., V. Hlavac, et al., Image Processing, Analysis, and Machine Vision. Thomson, 3 ed., 2008.

[27] Favaro, M., Color and depth based image segmentation using a game-theoretic approach, M.S. Thesis, Padua University, 2012.

[28] Park, S. Y. and Y. H. Lee, “Double smoothing of images using median and wiener filters,” IEEE Transactions on Acoustics, Speech and Signal Processing, vol. 37, no. 6, 1989.

[29] Gonzalez, R. C. and R. E. Woods, Digital Image Processing, ch. 10. Boston, MA, USA: Addison-Wesley Longman Publishing Co., Inc., 2nd ed., 2001.

[30] Kass, M., A. Witkin, et al., “Snakes: Active contour models,” International Journal Computer Vision, pp. 321–331, 1988.

[31] Pham, D. L., Ch. Xu, et al., "A Survey of Current Methods in Medical Image Segmentation", Annual Review of Biomedical Engineering, January 19, 1998.

[32] Bakoš, M., "Active Contours and their Utilization at Image Segmentation", Slovak Scientific grant agency VEGA funded project 1/2185, 2005.

[33] Osher, S. and J. A. Sethian, “Fronts propagating with curvature-dependent speed: Algorithm based on Hamilton-Jacobi formulations,” J. Comput Phys., vol. 79, pp. 12–49, 1988.

[34] Chan, T. F. and L. A. Vese, “Active contours without edges,” IEEE Trans. Image Process., vol. 10, no. 2, pp. 266–277, Feb. 2001.

[35] Sethian, J., “Level Set Methods and Fast Marching Methods,” Cambridge, U.K, Cambridge Univ. Press, 271-291, 1999.

[36] Osher, S., Fedkiw, R., “Level Set Methods and Dynamic Implicit Surfaces,” New York, Springer-Verlag, 1-23, 2002.

[37] Sussman, M., Smereka, P., et al., “A level set approach for computing solutions to incompressible two-phase flow,” J. Comput. Phys., 114(1): 146–159, 1994.

[38] Sussman, M., Fatemi, E., “An efficient, interface-preserving level set redistancing algorithm and its application to interfacial incompressible fluid flow,” SIAM J. Sci. Comput., 20(4): 1165–1191, 1999.

[39] Ferreira, P.M.M., Contributions to the segmentation of dermoscopic images, M.S. Thesis, Porto University, 2012.

[40] Lee, C. P., Robust Image Segmentation using Active Contours: Level Set Approaches, Ph.D. Thesis, North Carolina State University, 2005.

[41] Dowell, M. And Platt, T., Partition of the Ocean into Ecological Provinces: Role of Ocean-Colour Radiometry, IOCCG Report Number 9, 2009.

[42] Zhu, W., Zeng, N. et al., "Sensitivity, Specificity, Accuracy, Associated Confidence Interval and ROC Analysis with Practical SAS® Implementations", SAS® and all other

SAS Institute Inc, USA, 2010.

[43] Hsieh M.TH, et al., "Automatic segmentation of meningioma from non-contrasted brain MRI integrating fuzzy clustering and region growing", BMC Medical Informatics and Decision Making 2011.